# Distributed Space-Time Cooperative Schemes for Underwater Acoustic Communications

Madhavan Vajapeyam, Urbashi Mitra
Communication Sciences Institute
University of Southern California
3740 McClintock Avenue, Los Angeles, 90089
Email: {vajapeya,ubli}@usc.edu

James Preisig
Dept. of Applied Ocean
Physics and Engineering
Woods Hole Oceanographic
Institution, Woods Hole, MA 02543
Email: jpreisig@whoi.edu

Milica Stojanovic
Massachusetts Institute of Technology
Cambridge, MA 02139
Email: millitsa@mit.edu

***Abstract*— In resource limited, large scale underwater sensor networks, cooperative communication over multiple hops offers opportunities to save power. Intermediate nodes between source and destination act as cooperative relays. Herein, protocols coupled with space-time block code (STBC) strategies are proposed and analyzed for distributed cooperative communication. Amplify-and-forward type protocols are considered, in which intermediate relays do not attempt to decode the information. The Alamouti-based cooperative scheme proposed in [1] for flat-fading channels is modified in order work in the presence of multipath, which is a main characteristic of underwater acoustic channels. A time-reversal distributed space-time block code (TR-DSTBC) is employed, which extends the classical TR-STBC approach from [2] to a cooperative communication scenario. We show that, just like in the multi-antenna STBC case, TR along with the orthogonality of the DSTBC essentially allows for decoupling of the vector ISI detection problem into separate scalar problems, and therefore significant complexity reduction.**

## I. Introduction

Underwater sensor networks form an emerging technology paradigm that promises to enable or enhance several key applications in oceanic research, such as [3] [4]: data collection, pollution monitoring, tactical surveillance and disaster prevention. In such networks, acoustic communications will be employed as radio waves propagate very poorly in water. [3], [5].

On the other hand, exploiting sensor cooperation for terrestrial communications has also attracted considerable recent attention, in order to increase reliability, coverage, throughput and capacity ( [6] and references therein). A common feature among many of these networks is their *multihop* nature: communication is performed between source and destination via intermediate terminals. This provides several advantages over single hop schemes [6]: a) combating the severe signal decay over long distances, and therefore, saving transmission power; b) providing signal paths between terminals which do not have a direct line of sight between them; and c) providing multiple communication links for applications with a high data rate requirement which cannot be satisfied via a single link.

[0]This research has been funded in part by one or more of the following grants or organizations: ONR N-000140410273, Center for Embedded Networked Systems (NSF STC CCR-01-20778), NSF ITR CCF-0313392, and the USC WISE Program

Multihop networks can also provide additional gains through *cooperation* between terminals. Recent information theoretic results show that cooperation can increase the overall capacity of these networks by taking advantage of their inherent richness in spatial diversity [7]. Hence, a natural way to exploit this diversity is via *Distributed Space-Time Block Coding* (DSTBC) originally proposed in [7]. The goal of a DSTBC-based protocol is to allow the cooperating terminals to act, from the destination point of view, as a multi-antenna array employing a well designed Space-Time Block Code (STBC) [8]. Several DSTBC schemes have been recently proposed [1], [7], [9].

The idea that DSTBC schemes could be applied to underwater networks suggests itself naturally. The underwater acoustic channel, however, poses extra difficulties to the design of such communication protocols. Typical major challenges posed by underwater channels are [3]: severe range-dependent attenuation, extensive multipath propagation and highly variable propagation delays (due to slow sound propagation).

In this work, we consider the problem of underwater communication between single source (S) and destination (D) terminals. Data is relayed in a multi-hop fashion, through intermediate sensor nodes placed between S and D. Communication protocols based on distributed space-time coding (DSTBC) are considered. The time reversal STBC (TR-STBC) approach proposed in [2] for co-located antennas, is extended to a distributed antenna scenario. We show that, just like in the STBC case [2], [10], TR along with the orthogonality of the DSTBC essentially allows for decoupling of a vector ISI detection problem into separate scalar problems, without loss of optimality (neglecting "border effects" [10]) and, therefore, significant complexity reduction.

This paper is organized as follows. Section II introduces the signal model and TR-DSTBC scheme for 2 relays. The robustness of the scheme to asynchronous relay operation is motivated in Section III. A generalization of the scheme to more than two relays is presented in Section IV, based on the rate 1/2 orthogonal STBC. The adopted underwater channel model is presented in Section V, which is based on [11], [12]. Simulation results are presented in Section VI, including a sensitivity analysis of the scheme under non-idealized channel

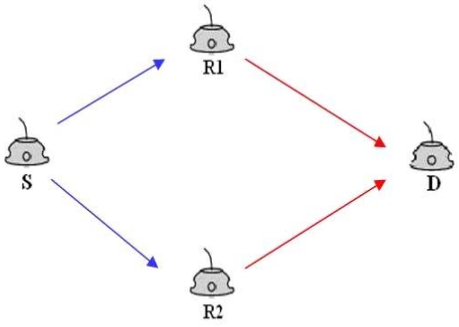


Fig. 1. 2 hop cooperative network.

conditions. Section VII presents the conclusions.

## II. Signal Model

We first consider the discrete-time signal model for a scenario with a single source terminal (S) communicating to a destination terminal (D) via a stage of two wireless relays as depicted in Figure 1. A generalization for more than two relays is given in Section IV.

Since the channels between the multiple links contain ISI, we will employ a discrete-time filter notation to represent them. To exemplify the notation, for a generic input $u(t)$ and channel filter $a(q^{-1})$ - with $q^{-1}$ denoting the delay operator - the output $v(t)$ is given by

$$v(t) = a(q^{-1})u(t) = \left(\sum_{i=0}^{L_c} a_i q^{-i}\right) u(t) = \sum_{i=0}^{L_c} a_i u(t-i), \quad t = 1, \ldots, N \quad (1)$$

where $L_c+1$ is the number of channel taps and $N$ is the block size. It is useful to note that

$$v(N-t+1) = a(q^{-1})u(N-t+1) = \left(\sum_{i=0}^{L_a} a_i q^{-i}\right) u(N-t+1) \quad t = 1, \ldots, N \quad (2)$$

Denoting by the time-reversed input and output by $\bar{u}(t) \triangleq u(N-t+1)$ and $\bar{v}(t) \triangleq v(N-t+1)$ respectively, we have from (2)

$$\bar{v}(t) = v(N-t+1) = a(q^{-1})u(N-t+1) = a(q)\bar{u}(t) \quad (3)$$

Let $h_i(q^{-1})$ and $g_i(q^{-1})$ denote the $S-R_i$ and $R_i-D$ channels respectively for a given relay $i$. Unless stated otherwise, we shall assume that all channels are independent, with taps that are independently fading and quasi-static (constant for a duration $2N$ plus any required guard bands, as explained next).

The source divides its transmission symbol stream $s(t)$ into two blocks $s_1(t)$ and $s_2(t)$, each of length $N$ and transmits them separated by a guard band to avoid interblock interference. For the same reason a preamble and a tail are inserted at the beginning and at the end of $s(t)$ respectively [10]. The received signal at $R_i$ at sampling times $t$ corresponding to the first transmission block is

$$r_{i,1}(t) = \sqrt{E_s} h_i(q^{-1}) s_1(t) + w_{i,1}(t), \quad t = 1, \ldots, N \quad (4)$$

and similarly for the second transmission block

$$r_{i,2}(t) = \sqrt{E_s} h_i(q^{-1}) s_2(t) + w_{i,2}(t), \quad t = 1, \ldots, N \quad (5)$$

Thus, $r_{i,k}(t)$ is the received signal at time $t$, at relay $i$ and block $k$, where $k = 1, 2$. The signal $s_k(t)$ is the $t$-th source transmitted symbol of block $k$ and can be taken from a PSK or QAM symbol constellation. The AWGN sequence $w_{i,k}(t)$ has unit variance. Furthermore, $w_{i,1}(t)$ and $w_{i,2}(t)$ are assumed to be independent. The energy per transmit symbol is denoted by $E_s$.

We assume, due to complexity and power limitations, that the relays can only perform Amplify and Forwarding type operations on their received signals (amplification, complex conjugation or time shift). No channel estimation or symbol detection is performed. In the case of flat fading, the work by Hua [1] has shown how an Alamouti-type processing can be employed by the relays to achieve diversity gains. We now describe its extension to multipath channels.

Both $R_1$ and $R_2$ transmit two blocks. Let $u_{i,k}(t)$ denote the signal transmitted by $R_i$ over block $k$ and time $t$. In the first block $R_1$ and $R_2$ transmit, respectively

$$u_{1,1}(t) = \sqrt{\frac{E_r}{K_1}} r_{1,1}(t) \quad (6)$$

$$u_{2,1}(t) = \sqrt{\frac{E_r}{K_2}} \bar{r}^*_{2,2}(t) \quad (7)$$

where $K_i, i = 1, 2$ is a normalizing factor applied to the received signal of relay $i$, to make it unit power, and $E_r$ is the transmit energy per symbol for each relay.

In the second block, the transmitted signals are

$$u_{1,2}(t) = \sqrt{\frac{E_r}{K_1}} r_{1,2}(t) \quad (8)$$

$$u_{2,2}(t) = -\sqrt{\frac{E_r}{K_2}} \bar{r}^*_{2,1}(t) \quad (9)$$

We note that only $R_2$ conjugates and time-reverses during both of its blocks. This is different from the approach in [2] where two co-located *antennas* perform conjugation and time-reversal over the second block. Although both approaches are equivalent for the STBC scenario, the latter would destroy the quasi-static channel assumption of the current DSTBC setting.

The received signal at the destination for block $k (k = 1, 2)$ is therefore given by

$$y_k(t) = g_1(q^{-1}) u_{1,k}(t) + g_2(q^{-1}) u_{2,k}(t) + n_k(t) \quad (10)$$

where $n_k(t)$ is the receiver AWGN with unit variance. Substituting the expressions for $u_{i,k}(t)$ from above we have

$$y_1(t) = \sqrt{\frac{E_s E_r}{K_1}} g_1(q^{-1}) h_1(q^{-1}) s_1(t) + \sqrt{\frac{E_s E_r}{K_2}} g_2(q^{-1}) h_2^*(q) \bar{s}_2^*(t) + n_1'(t) \quad (11)$$

$$y_2(t) = \sqrt{\frac{E_s E_r}{K_1}} g_1(q^{-1}) h_1(q^{-1}) s_2(t) - \sqrt{\frac{E_s E_r}{K_2}} g_2(q^{-1}) h_2^*(q) \bar{s}_1^*(t) + n_2'(t) \quad (12)$$

where

$$n_k'(t) = n_k(t) + \sqrt{\frac{E_r}{K_1}} g_1(q^{-1}) w_{1,k}(t) + \sqrt{\frac{E_r}{K_2}} g_2(q^{-1}) \bar{w}_{2,k}^*(t) \quad (13)$$

It follows, therefore, that the PSD of $n_i'(t)$, denoted by $X(q^{-1}, q)$ is given by

$$X(q^{-1}, q) = 1 + \frac{E_r}{K_1} g_1(q^{-1}) g_1^*(q) + \frac{E_r}{K_2} g_2(q^{-1}) g_2^*(q) \quad (14)$$

where we keep the PSD notation in the $q$ domain instead of switching to the more conventional domain $z$, for notation simplicity.

By computing the time reversal and conjugation of $y_2(t)$ and defining $\mathbf{y}(t) = [y_1(t) \quad \bar{y}_2^*(t)]^T$ we obtain

$$\mathbf{y}(t) = \mathbf{H}(q^{-1}, q) \begin{bmatrix} s_1(t) \\ \bar{s}_2^*(t) \end{bmatrix} + \begin{bmatrix} n_1'(t) \\ \tilde{n}_2(t) \end{bmatrix} \quad (15)$$

where $\tilde{n}_2^* = \bar{n}_2'$ and the equivalent $S - D$ channel matrix is

$$\mathbf{H}(q^{-1}, q) \triangleq \begin{bmatrix} \sqrt{\frac{E}{K_1}} g_1(q^{-1}) h_1(q^{-1}) & \sqrt{\frac{E}{K_2}} g_2(q^{-1}) h_2^*(q) \\ -\sqrt{\frac{E}{K_2}} g_2^*(q) h_2(q^{-1}) & \sqrt{\frac{E}{K_1}} g_1^*(q) h_1^*(q) \end{bmatrix} \quad (16)$$

where $E \triangleq E_s E_r$. Note that the special case of flat fading S-R and R-D channels and $K_1 = K_2 = K$ corresponds to the channel matrix

$$\mathbf{H} = \sqrt{\frac{E}{K}} \begin{bmatrix} g_1 h_1 & g_2 h_2^* \\ -g_2^* h_2 & g_1^* h_1^* \end{bmatrix} \quad (17)$$

which has an Alamouti [13] structure, as observed in [1].

Since we assume perfect CSI at the receiver, it can process $\mathbf{y}(t)$ given by (15) with the matched filter $\mathbf{H}^H(q^{-1}, q)$. Due to the orthogonality of $\mathbf{H}(q^{-1}, q)$, we have

$$\mathbf{H}^H(q^{-1}, q) \mathbf{H}(q^{-1}, q) \triangleq \mathbf{f}(q^{-1}) \mathbf{f}^*(q) \mathbf{I} \quad (18)$$

where $\mathbf{I}$ is the identity matrix and we define the factorization

$$\mathbf{f}(q^{-1}) \mathbf{f}^*(q) = \left( \sum_{i=1}^{2} \frac{E_s E_r}{K_i} g_i^*(q) g_i(q^{-1}) h_i^*(q) h_i(q^{-1}) \right) \quad (19)$$

The matched filter output vector is given by

$$\mathbf{z}(t) \triangleq \mathbf{H}^H(q^{-1}, q) \mathbf{y}(t) \quad (20)$$

whose components can be expressed as

$$z_1(t) = \mathbf{f}(q^{-1}) \mathbf{f}^*(q) s_1(t) + v_1(t) \quad (21)$$

$$z_2(t) = \mathbf{f}(q^{-1}) \mathbf{f}^*(q) \bar{s}_2^*(t) + v_2(t) \quad (22)$$

and the output noise $\mathbf{v}(t) \triangleq [v_1(t) \quad v_2(t)]^T$ has PSD

$$X_{\mathbf{v}}(q^{-1}, q) = X(q^{-1}, q) \mathbf{f}(q^{-1}) \mathbf{f}^*(q) \mathbf{I} \quad (23)$$

Thus, $v_1(t)$ and $v_2(t)$ are independent and the problem of jointly detecting $s_1(t)$ and $s_2(t)$ from $\mathbf{z}(t)$ decouples: $s_1(t)$ is detected from $z_1(t)$ and $s_2(t)$ from $z_2(t)$.

Comparing matched filter outputs given by (39) and (22) with the equivalent STBC relations for 2 antennas in [2] we note two key differences. First, the noise PSD given by (23) contains a term $X(q^{-1}, q) \neq 1$ due to the noise amplification at the relays. This noise is also colored, since the R-D channel introduces ISI. Second, the channel $\mathbf{f}(q^{-1})$ accounts for the overall effect of the "product" channels $g_i(q^{-1}) h_i(q^{-1})$, which increases ISI and results in non-Gaussian its statistical properties.

Since perfect receiver CSI is assumed, we can employ the spectral factorization $X(q^{-1}, q) = \mathbf{x}(q) \mathbf{x}(q^{-1})$ and, hence, whiten the noise by applying the filter $W(q^{-1}, q) = \frac{1}{\mathbf{x}(q^{-1}) \mathbf{f}^*(q)}$, resulting in the desired AWGN model

$$\tilde{z}_1(t) = \frac{\mathbf{f}(q^{-1})}{\mathbf{x}(q^{-1})} s_1(t) + \tilde{v}_1(t) \approx \tilde{\mathbf{h}}(q^{-1}) s_1(t) + \tilde{v}_1(t) \quad (24)$$

$$\tilde{z}_2(t) = \frac{\mathbf{f}(q^{-1})}{\mathbf{x}(q^{-1})} \bar{s}_2^*(t) + \tilde{v}_2(t) \approx \tilde{\mathbf{h}}(q^{-1}) \bar{s}_2^*(t) + \tilde{v}_1(t) \quad (25)$$

where $\tilde{\mathbf{h}}(q^{-1})$ denotes the least square FIR approximation of $\mathbf{h}(q^{-1}) \triangleq \frac{\mathbf{f}(q^{-1})}{\mathbf{x}(q^{-1})}$. Denoting respectively by $L_f$, $L_x$ and $L_{\tilde{h}}$ the number of taps in $\mathbf{f}$, $\mathbf{x}$ and $\tilde{\mathbf{h}}$, we set $L_{\tilde{h}} = L_f + L_x - 1$. For simulation purposes, we shall assume that this approximation incurs negligible error compared to the desired filter response.

For the FIR model in (24) and (25), maximum likelihood sequence estimation (MLSE) can be carried out via a Viterbi-type algorithm [14]. For channels experiencing extensive multipath however (such as the underwater channels), the MLSE detector can be prohibitively complex, and a decision-feedback equalizer (DFE) has been shown to yield good results in practice [15].

## III. Coping with imperfect relay synchronization

The distributed nature of the cooperative communication strategy described in section II naturally brings up the question of whether the relays need to operate under perfect synchronization. Indeed, this is a common assumption in several recently proposed distributed cooperation strategies [1] [16] [9].

In many practical situations, however, due to different delays between the cooperative nodes and the destination, achieving perfect synchronization can be very difficult [17]. The long sound propagation delays in underwater networks can, therefore, potentially increase this problem.

A direct consequence of imperfect synchronization between relays is the the introduction of time dispersion in the channels even in frequency flat channels [17] [18] which is due to imperfect sampling times at the receiver. Intuitively, therefore, the TR-DSTBC approach for frequency selective channels can also operate with asynchronous relays, if we assume a known upper bound on the relative transmission delays (to avoid interblock interference).

From the received signal model at the relays given by (4) and (5), the received signal for block $k$ at D assuming a time delay of $\epsilon$ between transmissions from $R_1$ and $R_2$ is

$$y_1(t) = \sqrt{\frac{E_s E_r}{K_1}} g_1(q^{-1}) h_1(q^{-1}) s_1(t) + \sqrt{\frac{E_s E_r}{K_2}} g_2(q^{-1}) h_2^*(q) R_{p_\epsilon}(q^{-1}, q) \bar{s}_2^*(t) + n_1'(t) \tag{26}$$

$$y_2(t) = \sqrt{\frac{E_s E_r}{K_1}} g_1(q^{-1}) h_1(q^{-1}) s_2(t) - \sqrt{\frac{E_s E_r}{K_2}} g_2(q^{-1}) h_2^*(q) R_{p_\epsilon}(q^{-1}, q) \bar{s}_1^*(t) + n_2'(t) \tag{27}$$

where $R_{p_\epsilon}(q^{-1}, q)$ denotes the transmit pulse correlation function for a delay $\epsilon$, with coefficients

$$R_{p_\epsilon}(k) = p(t+\epsilon) * p(-t)|_{t=kT}, \qquad -\infty < k < \infty \tag{28}$$

and $p(t)$ denotes the transmit pulse shape, usually of raised cosine characteristic and unit energy. Hence, in a perfectly synchronized scenario, $R_{p_0}(q^{-1}, q) = 1$.

Clearly, from (26) and (27) the imperfect synchronization increases the dispersion of the $R_2$-D channel. However, defining an equivalent channel $h_2'(q^{-1}) \triangleq R_{p_\epsilon}(q^{-1}, q) h_2(q^{-1})$ an identical form of the signal model in (15) is obtained, with $h_2'(q^{-1})$ replacing $h_2(q^{-1})$. Thus, the TR-DSTBC formulation can conveniently address the case of asynchronous relays by simple generalization of the channel model.

## IV. Extension to more than two relays

The key property that allows signal decoupling at receiver for the two-relay scheme presented in section II is the orthogonality of the Alamouti STBC. It allows two signal streams to be transmitted via two relays over two blocks of time, and, hence, exhibits full rate of one.

Unfortunately, no full rate orthogonal STBC exists (for complex modulation) for more than two antennas [8]. In this section we present a generalization of the two relay scheme for two hops presented earlier to arbitrary number of relays based on rate 1/2 orthogonal STBCs [8], denoted by TR-1/2. For simplicity we describe the TR-1/2 scheme for the case of 4 relays. The extension to arbitrary number of relays is intuitive.

The information stream $d(t)$ is now divided into four equal length blocks $d_1(t), ..., d_4(t)$. The source transmission occurs over *eight* blocks: in the first four blocks,

$$s_k(t) = \sqrt{E_s} d_k(t), k = 1, \ldots, 4 \tag{29}$$

are transmitted; in the last four blocks,

$$s_k(t) = \sqrt{E_s} \bar{d}_{k-4}^*(t), k = 5, \ldots, 8 \tag{30}$$

are sent. Note that the blocks of the second half transmission are the time-reversed conjugates of the first half blocks. Hence the rate of the scheme is 1/2.

The received signals at relay $i, i = 1, \ldots, 4$ and block $k$, $k, i = 1, ..., 8$ are

$$r_{i,k}(t) = \sqrt{E_s} h_i(q^{-1}) s_k(t) + w_{i,k}(t), \quad t = 1, \ldots, N \tag{31}$$

where, as before, the $h_i(q^{-1})$ denotes the channel coefficients between source and relay $i$ and $w_{i,k}(t)$ is AWGN. The processing performed by each relay over its received blocks is dictated by the underlying rate 1/2 STBC structure. In general for symbols $x_i, i = 1, \ldots, 4$ from a complex alphabet, the rate 1/2 STBC is

$$\mathbf{S} = \begin{bmatrix} S \\ S^* \end{bmatrix} \quad \text{where } S = \begin{bmatrix} x_1 & x_2 & x_3 & x_4 \\ -x_2 & x_1 & -x_4 & x_3 \\ -x_3 & x_4 & x_1 & -x_2 \\ -x_4 & -x_3 & x_2 & x_1 \end{bmatrix} \tag{32}$$

Thus, if each relay corresponds to a different column of $\mathbf{S}$, and each row to a different time block, the relay transmissions can be represented by the matrix

$$U \triangleq \begin{bmatrix} \mathbf{u}_1(t) & \mathbf{u}_2(t) & \mathbf{u}_3(t) & \mathbf{u}_4(t) \end{bmatrix} \triangleq \sqrt{\frac{E_r}{K}} \begin{bmatrix} r_{1,1}(t) & r_{2,2}(t) & r_{3,3}(t) & r_{4,4}(t) \\ -r_{1,2}(t) & r_{2,1}(t) & -r_{3,4}(t) & r_{4,3}(t) \\ -r_{1,3}(t) & r_{2,4}(t) & r_{3,1}(t) & -r_{4,2}(t) \\ -r_{1,4}(t) & -r_{2,3}(t) & r_{3,2}(t) & r_{4,1}(t) \\ r_{1,5}(t) & r_{2,6}(t) & r_{3,7}(t) & r_{4,8}(t) \\ -r_{1,6}(t) & r_{2,5}(t) & -r_{3,8}(t) & r_{4,7}(t) \\ -r_{1,7}(t) & r_{2,8}(t) & r_{3,5}(t) & -r_{4,6}(t) \\ -r_{1,8}(t) & -r_{2,7}(t) & r_{3,6}(t) & r_{4,5}(t) \end{bmatrix} \tag{33}$$

where $K_1 = \ldots = K_4 = K$ is assumed for simplicity and each column $\mathbf{u}_i(t) = [u_{i,1}(t), \ldots, u_{i,8}(t)]^T$ consists of the transmission of 8 blocks, according to (33) and (31).

Denoting by $g_i(q^{-1})$ the channels from relay $i$ to destination, the received signal at destination (after time reversing

and conjugating the second-half received blocks) is

$$\mathbf{y}(t) = \begin{bmatrix} \sum_{i=1}^{4} w_{i,1}(t) g_i(q^{-1}) + \eta_1(t) \\ \vdots \\ \sum_{i=1}^{4} w_{i,4}(t) g_i(q^{-1}) + \eta_4(t) \\ \sum_{i=1}^{4} \bar{w}^*_{i,5}(t) g_i(q^{-1}) + \bar{\eta}^*_5(t) \\ \vdots \\ \sum_{i=1}^{4} \bar{w}^*_{i,8}(t) g_i(q^{-1}) + \bar{\eta}^*_8(t) \end{bmatrix} + \begin{bmatrix} f_1(q^{-1}) & f_2(q^{-1}) & f_3(q^{-1}) & f_4(q^{-1}) \\ f_2(q^{-1}) & -f_1(q^{-1}) & f_4(q^{-1}) & -f_3(q^{-1}) \\ -f_3(q^{-1}) & f_4(q^{-1}) & f_1(q^{-1}) & -f_2(q^{-1}) \\ -f_4(q^{-1}) & -f_3(q^{-1}) & f_2(q^{-1}) & f_1(q^{-1}) \\ f_1^*(q) & f_2^*(q) & f_3^*(q) & f_4^*(q) \\ f_2^*(q) & -f_1^*(q) & f_4^*(q) & -f_3^*(q) \\ -f_3^*(q) & f_4^*(q) & f_1^*(q) & -f_2^*(q) \\ -f_4^*(q) & -f_3^*(q) & f_2^*(q) & f_1^*(q) \end{bmatrix} \begin{bmatrix} d_1(t) \\ d_2(t) \\ d_3(t) \\ d_4(t) \end{bmatrix} \tag{34}$$

where $\eta_k(t)$ is additive white noise at the receiver and $f_i(q^{-1}) = \sqrt{\frac{E_s E_r}{K}} h_i(q^{-1}) g_i(q^{-1})$ is the overall channel S-$R_i$-D.

Just as in the 2-relay case, we can define the channel matrix

$$\mathbf{H}(q^{-1}, q) \triangleq \begin{bmatrix} f_1(q^{-1}) & f_2(q^{-1}) & f_3(q^{-1}) & f_4(q^{-1}) \\ f_2(q^{-1}) & -f_1(q^{-1}) & f_4(q^{-1}) & -f_3(q^{-1}) \\ -f_3(q^{-1}) & f_4(q^{-1}) & f_1(q^{-1}) & -f_2(q^{-1}) \\ -f_4(q^{-1}) & -f_3(q^{-1}) & f_2(q^{-1}) & f_1(q^{-1}) \\ f_1^*(q) & f_2^*(q) & f_3^*(q) & f_4^*(q) \\ f_2^*(q) & -f_1^*(q) & f_4^*(q) & -f_3^*(q) \\ -f_3^*(q) & f_4^*(q) & f_1^*(q) & -f_2^*(q) \\ -f_4^*(q) & -f_3^*(q) & f_2^*(q) & f_1^*(q) \end{bmatrix} \tag{35}$$

which satisfies

$$\mathbf{H}^H(q^{-1}, q)\mathbf{H}(q^{-1}, q) \triangleq \mathbf{f}(q^{-1})\mathbf{f}^*(q)\mathbf{I} \tag{36}$$

with

$$\mathbf{f}(q^{-1})\mathbf{f}^*(q) = \left( 2 \sum_{i=1}^{4} \sqrt{\frac{E_s E_r}{K_i}} g_i(q^{-1}) g_i^*(q) h_i(q^{-1}) h_i^*(q) \right) \mathbf{I} \tag{37}$$

and, hence, is orthogonal.

The matched filter output vector is given by

$$\mathbf{z}(t) \triangleq \mathbf{H}^H(q^{-1}, q)\mathbf{y}(t) \tag{38}$$

consisting of 4 blocks, each one given by

$$z_i(t) = \mathbf{f}(q^{-1})\mathbf{f}^*(q) d_i(t) + v_i(t), i = 1, \ldots, 4 \tag{39}$$

and the output noise $\mathbf{v}(t) \triangleq [v_1(t), \ldots, v_4(t)]^T$ has PSD

$$X_{\mathbf{v}}(q^{-1}, q) = X(q^{-1}, q)\mathbf{f}(q^{-1})\mathbf{f}^*(q)\mathbf{I} \tag{40}$$

Hence, $v_1(t), \ldots, v_4(t)$ are independent and the problem of jointly detecting $d_i(t), i = 1, \ldots, 4$ from $\mathbf{z}(t)$ again decouples, just like in the 2-relay case.

It turns out that [8]: i) a rate 1/2 complex orthogonal design exists for any size $2n \times n$ where $n$ is a power of two; ii) an orthogonal design of size $l \times n$ where $l < n$, can be obtained by deleting $n - l$ columns of the $2n \times n$ design. Hence, the TR-1/2 scheme can be generalized to any number of relays in straightforward fashion.

## V. Underwater Channel Model

We adopt a geometry-based multipath model similar to [11], [12]. All paths in individual S-R or R-D links are assumed to be independent and Rayleigh fading. The main difference in our model is that we assume multipath components are fading. As is common in this case, we consider a quasi-static fading model, in which the channel is constant within a fixed duration and changes to an independent realization over the next time frame. We analyze the effects of a slowly time varying channel within the frame as well as non-perfect CSI via simulations in the next section.

A given multipath arrival $p$ is characterized by its mean magnitude gain $\alpha_p$ and delay $t_p$. These quantities are dependent on the path length $l_p$, which in turn is a function of the given range $R$. The path magnitude gain is given by $\alpha_p = \frac{\Gamma_p}{\sqrt{A(l_p)}}$, where $\Gamma_p, \Gamma_p \leq 1$ is the amount of loss due to reflection at the bottom and surface. The acoustic propagation loss, represented by $A(l_p)$ is given by

$$A(l_p) = l_p^k [a(f_c)]^{l_p} \tag{41}$$

where $k = 1.5$ for practical spreading, $f_c$ is the carrier frequency and absorbtion coefficient $a(f_c)$ (in dB/Km) given by Thorp's formula

$$10 \log a(l_p) = \frac{0.11 f_c^2}{1 + f_c^2} + \frac{44 f_c^2}{4100 + f_c^2} + 2.75.10^{-4} f_c^2 + 0.003 \tag{42}$$

Finally, the path delay is given by $t_p = l_p / c$, where $c = 1500$ m/s is the speed of sound.

Figure 2 shows the channel path delays and magnitudes for a distance of 3 Km between transmitter and receiver, $f_c = 15$ KHz and depth of 75 m.

## VI. Simulation Results

For simulation purposes, we consider an underwater network with S-D distance of 6 Km, carrier frequency $f_c = 15$ KHz and channel depth of 75 m. Three communication strategies are compared: single hop, where the source communicates directly to the destination; and cooperative (2 hop) with either 2 or 4 relays, as described in Sections II and IV. The modulation is BPSK with a symbol duration of $T = 2.5$ ms and, therefore, a data rate of 400 b/s. Our first goal is to compare the performance of the MLSE and DFE. Hence, the data rate is deliberately low in order to limit the ISI span to only a few symbols and thus simplify the MLSE. Multipath components present beyond $5T$ are, therefore, neglected. This results in a channel with 2 taps per hop in the cooperative strategy, and 3 taps for the direct communication approach. In the latter case, multipath arrivals can occur within a fraction of a symbol time. In this case these arrivals can add up constructively [12], and thus result in a stronger path, or

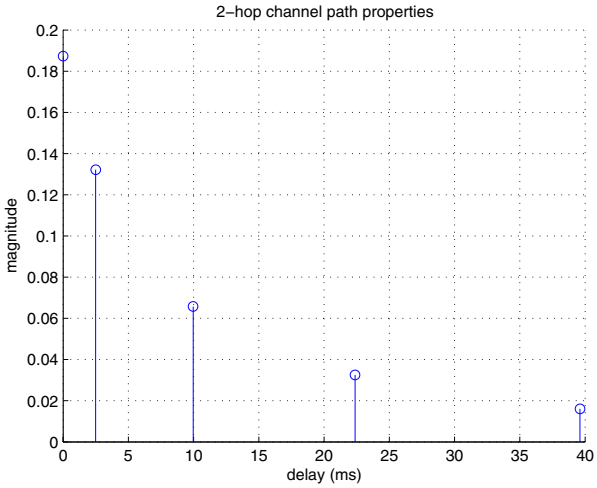


Fig. 2. 2 hop channel profile: range = 3 Km, $f_c = 15KHz$, depth = 75m

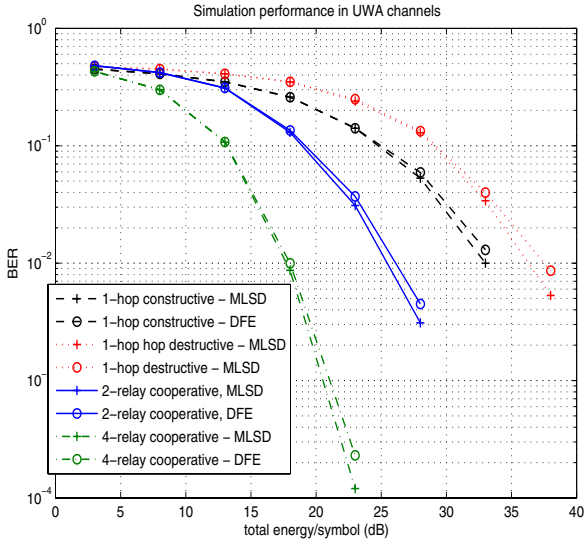


Fig. 3. TR-DSTBC performance: range = 6 Km, $f_c = 15KHz$, depth = 75m

destructively [19], weakening the resulting overall multipath component. We consider both scenarios separately here.

Figure 3 shows the performance of the MLSD and DFE approaches for the cooperative and single hop strategies. For the DFE, the number of feedforward and feedback filter taps is $N_1 + 1 = 15$ and $N_2 = L_c$ respectively, where $L_c + 1$ is the number of taps of the overall S-D channel. It is clear for all cases considered that the DFE performance is very close to MLSD. Furthermore, the results highlight the significant performance improvement introduced by cooperation. The two main reasons are: a) multi-hoping gain, since the overall attenuation suffered by the signal is less severe; b) spatial diversity gain, which is due to the spatial diversity inherently available in the distributed network, which is exploited via distributed space-time processing.

Note that, although both the single-hop and 2-hop cooperative communication approaches can yield diversity gain through multipath combining, only the latter provides further gains through spatial diversity. This explains the larger decay slope of the error probability curves for the cooperative schemes.

Finally, we note that increasing the number of cooperating relays further increases the available spatial diversity in the system and, hence, further improves the performance. This can also be verified for the 4-relay case in Figure 3, which employs the TR-1/2 scheme.

### *A. Sensitivity to imperfect CSI*

In a practical scenario, the receiver does not have perfect knowledge of the channel. Due to the presence of channel estimation errors, a degradation in the idealized performance results is naturally expected. In this section, we assess, via simulations, the performance of the receiver employing a DFE under different imperfect CSI conditions.

We model the channel estimation error as a random error matrix that is added to the true channel matrix $\mathbf{H}(q^{-1}, q)$. The estimated channel matrix $\hat{\mathbf{H}}(q^{-1}, q)$, is given by

$$\hat{\mathbf{H}}(q^{-1}, q) = \mathbf{H}(q^{-1}, q) + \mathbf{E}(q^{-1}, q) \tag{43}$$

with $\mathbf{E}(q^{-1}, q)$ expressed as

$$\mathbf{E}(q^{-1}, q) = \begin{bmatrix} E_{11}(q^{-1}, q) & E_{12}(q^{-1}, q) \\ E_{21}(q^{-1}, q) & E_{22}(q^{-1}, q) \end{bmatrix} \tag{44}$$

In terms of the actual channel estimates $\hat{g}_i(q^{-1}, q)$ and $\hat{h}_i(q^{-1}, q)$, we can also write

$$\hat{\mathbf{H}}(q^{-1}, q) \triangleq \begin{bmatrix} \hat{g}_1(q^{-1})\hat{h}_1(q^{-1}) & \hat{g}_2(q^{-1})\hat{h}_2^*(q) \\ -\hat{g}_2^*(q)\hat{h}_2(q^{-1}) & \hat{g}_1^*(q)\hat{h}_1^*(q) \end{bmatrix} \tag{45}$$

where the constant terms $\sqrt{E_s E_r / K_i}$ are now incorporated into the channels, for notational simplicity. The channel estimates are given by

$$\hat{h}_i(q^{-1}) = h_i(q^{-1}) + e_{h_i}(q^{-1}) \tag{46}$$

$$\hat{g}_i(q^{-1}) = g_i(q^{-1}) + e_{g_i}(q^{-1}) \tag{47}$$

Hence, we can write

$$E_{11}(q^{-1}, q) = e_{h_1}(q^{-1}) \left(e_{g_1}(q^{-1}) + g_1(q^{-1})\right) + e_{g_1}(q^{-1}) h_1(q^{-1}) \tag{48}$$

$$E_{12}(q^{-1}, q) = e_{h_2}^*(q) \left(e_{g_2}(q^{-1}) + g_2(q^{-1})\right) + e_{g_2}(q^{-1}) h_2^*(q) \tag{49}$$

$$E_{21}(q^{-1}, q) = -e_{h_2}(q^{-1}) \left(e_{g_2}^*(q) + g_2^*(q)\right) - e_{g_2}^*(q) h_2(q^{-1}) \tag{50}$$

$$E_{22}(q^{-1}, q) = e_{h_1}^*(q) \left(e_{g_2}(q^{-1}) + g_1^*(q)\right) + e_{g_1}^*(q) h_1^*(q) \tag{51}$$

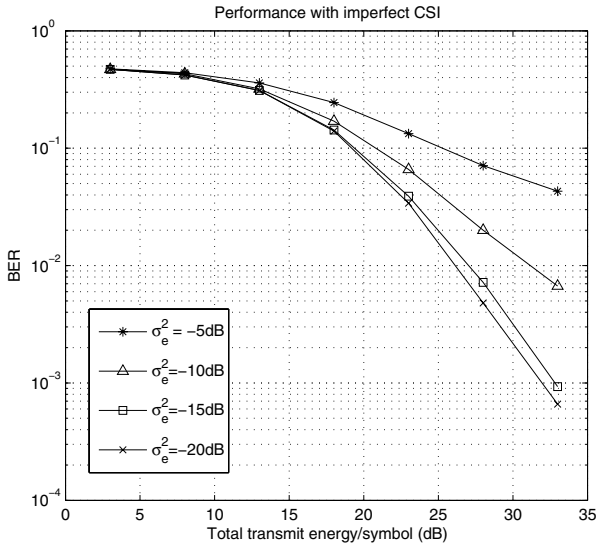


Fig. 4. TR-DSTBC: sensitivity to channel estimation errors

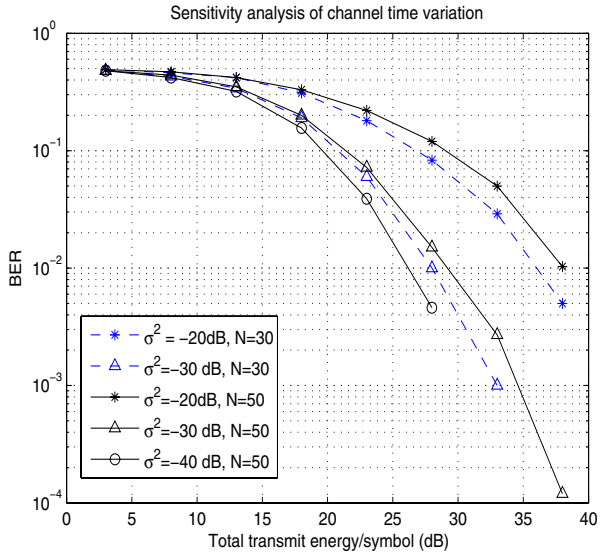


Fig. 5. TR-DSTBC: sensitivity to channel time variations

The matched-filter processing in (20) is now performed using the channel estimate $\hat{\mathbf{H}}(q^{-1},q)$. From (15) and (20),

$$\hat{\mathbf{z}}(t) = \hat{\mathbf{H}}^H(q^{-1},q)\mathbf{y}(t) = \mathbf{z}(t) + \mathbf{E}^H(q^{-1},q)\mathbf{H}(q^{-1},q)\begin{bmatrix} s_1(t) \\ \bar{s}_2^*(t) \end{bmatrix} + \mathbf{E}^H(q^{-1},q)\begin{bmatrix} \eta_1'(t) \\ \tilde{\eta}_2(t) \end{bmatrix} \quad (52)$$

Assuming $s_1(t)$ is to be detected, we notice from (52) that the imperfect CSI incurs not only in noise enhancement of the decision statistic, but also self and inter block interference from $s_1(t)$ and $s_2(t)$ respectively.

Figure 4 shows the performance sensitivity of the 2-relay scheme for imperfect CSI. The estimation error in each path $p$ for all channels is assumed to be zero mean, complex Gaussian with variance $\sigma_{e_p}^2 = \sigma_e^2\sigma_p^2$, where $\sigma_p^2$ is the mean square magnitude of path $p$. For $\sigma_e^2 = 20$ dB, the degradation from perfect CSI is very small and it deteriorates rather gracefully with increasing $\sigma_e^2$. As expected, for large estimation errors the system cannot take full advantage of the spatial diversity, and significant performance deterioration occurs.

### *B. Sensitivity to channel time variations*

To investigate the performance of the system with channel time variations, we assume a first order time-varying model for each path of the overall channel $\mathbf{f}$ in the model derived in (39) and (22). Hence, the matched filter outputs are

$$z_1(t) = \mathbf{f}(q^{-1},t)\mathbf{f}^*(q,t)s_1(t) + v_1(t) \quad (53)$$

$$z_2(t) = \mathbf{f}(q^{-1},t)\mathbf{f}^*(q,t)\bar{s}_2^*(t) + v_2(t) \quad (54)$$

An first-order autoregressive (AR) model is assumed for each of the tap coefficients of the filter $\mathbf{f}$. A similar approach to model channel time variation characteristics was also employed in [20]. Each tap $f_i$ is modelled as

$$f_i(t) = \sigma f_i(t-1) + \sqrt{1-\sigma^2}\epsilon(t) \quad (55)$$

where $\epsilon(t)$ is a complex white Gaussian innovation process of unit variance. For a symbol rate $f_s$, we can relate the Doppler spread and the AR parameter $\sigma$ as [20]

$$\sigma = 2 - \cos(w_d/2) - \sqrt{\cos^2(w_d/2) - 4\cos(w_d/2) + 3} \quad (56)$$

Figure 5 shows the performance of the scheme under several time varying conditions, controlled by the parameter $\sigma$. Two types of frame length were used: 50 and 30 symbols. For $N = 50$ the time variations accumulated across the frame incurs a slightly more severe degradation compared to a $N = 30$ frame. In both cases, most of the performance gains are still observed for channel variations on the range of $\sigma = -40$dB to -30dB.

## VII. Conclusions

In this paper, cooperative protocols for distributed space-time communications in underwater networks were proposed and analyzed. It was shown that, extending the time-reversal STBC idea originally proposed for multiple antenna systems, the cooperative schemes can achieve significant performance improvement in multipath channels. The TR-DSTBC approach has the added advantage of not requiring a computationally expensive multidimensional equalization at the receiver.

## References

[1] Y. Hua, Y. Mei, and Y. Chang, "Wireless antennas making wireless communications perform like wireline communications," in *Proc of IEEE Topical Conference on Wireless Communication Technology*, Honolulu, Hawaii, October 15-17 2003.

[2] E. Lindskog and A. Paulraj, "A transmit diversity scheme for channels with intersymbol interference," in *Proc of ICC 2000*, pp. 307–311, June 18–22 2000.

[3] I. F. Akyildiz, D. Pompili, and T. Melodia, "Underwater acoustic sensor networks: Research challenges," *Elsevier's Journal of Ad Hoc Networks*, vol. 3, no. 3, pp. 257–279, 2005.

[4] E. M. Sozer, M. Stojanovic, and J. G. Proakis, "Underwater acoustic networks," *IEEE Journal of Oceanic Engineering*, vol. 25.

[5] M. Stojanovic, "Recent advances in high-speed underwater acoustic communications," *IEEE Journal of Oceanic Engineering*, vol. 21, no. 2, pp. 125–136, 1996.
[6] H. Gharavi and K. Ban, "Multihop sensor network design for wide-band communications," *Proceedings of the IEEE*, vol. 91.
[7] J. Laneman and G. W. Wornell, "Distributed space-time coded protocols for exploiting cooperative diversity in wireless networks," *IEEE Trans. on Information. Theory*, vol. 49.
[8] V. Tarokh, H. Jafarkhani, and A. R. Calderbank, "Space-time block codes from orthogonal designs," *IEEE Transactions on Information Theory*, vol. 45, pp. 1456–67, June 1999.
[9] R. U. Nabar, H. Bolcskei, and F. W. Kneubuhler, "Fading relay channels: Performance limits and space-time signal design," *IEEE Journal on Selected Areas in Communications*, vol. 22, August 2004.
[10] E. Larsson, P. Stoica, E. Lindskog, and J. Li, "Space-time block coding for frequency-selective channels," in *Proc of ICASSP 2002*, vol. 3, pp. 2405–2408, May 13–17 2002.
[11] M. Stojanovic, "Retrofocussing techniques for high rate acoustic communications," *Journal of the Acoustical Society of America*, vol. 117, pp. 1173–1185, March 2005.
[12] A. Zielinski, Y.-H. Yoon, and L. Wu, "Performance analysis of digital acoustic communication in a shallow water channel," *IEEE Journal of Oceanic Engineering*, vol. 20, pp. 293–299, October 1995.
[13] S. M. Alamouti, "A simple transmit diversity technique for wireless communications," *IEEE Trans. on Select Areas in Comm.*, vol. 16, pp. 1451–58, October 1998.
[14] J. Proakis, *Digital Communications*. New York: McGraw Hill, 1995.
[15] M. Stojanovic, L. Freitag, and M. Johnson, "Channel-estimation-based adaptive equalization of underwater acoustic signals," in *Proc of OCEANS'99*, vol. 2.
[16] A. Sendonaris, E. Erkip, and B. Aazhang, "User cooperation diversity - part 1:system description," *IEEE Trans. on Comm.*, vol. 51, pp. 1927–1938, November 2003.
[17] X. E. Li, "Space-time coded multi-transmission among distributed transmitters without perfect synchronization," *IEEE Signal Processing Letters*, vol. 11, pp. 948–951, December 2004.
[18] Y. Mei, Y. Hua, A. Swami, and B. Daneshrad, "Combating synchronization errors in cooperative relays," in *Proceedings of IEEE International Conference on Acoustics, Speech and Signal Processing ICASSP'05*, pp. 369–372, Philadelphia.
[19] M. Chitre, J. Potter, and O. S. Heng, "Underwater acoustic channel characterisation for medium-range shallow water communications," in *Proc of OCEANS'04*, vol. 1.
[20] T. H. Eggen, A. B. Baggeroer, and J. C. Preisig, "Communication over Doppler spread channels - part I: Channel and receiver presentation," *IEEE Journal of Oceanic Engineering*, vol. 25, pp. 62–71, January 2000.